Talanta 128 (2014) 31–37

Contents lists available at ScienceDirect

Talanta

journal homepage: www.elsevier.com/locate/talanta

Nano sponge Mn_2O_3 as a new adsorbent for the preconcentration of Pd(II) and Rh(III) ions in sea water, wastewater, rock, street sediment and catalytic converter samples prior to FAAS determinations

Emre Yavuz, Şerife Tokalıoğlu *, Halil Şahan, Şaban Patat

Erciyes University, Faculty of Science, Chemistry Department, TR-38039 Kayseri, Turkey

ARTICLE INFO

Article history:
Received 11 January 2014
Received in revised form
17 April 2014
Accepted 18 April 2014
Available online 26 April 2014

Keywords:
Nano-sponge manganese oxide
Palladium
Rhodium
Solid phase extraction
Rapid kinetic
Atomic absorption spectrometry

ABSTRACT

In this study, a nano sponge Mn_2O_3 adsorbent was synthesized and was used for the first time. Various parameters affecting the recovery values of Pd(II) and Rh(III) were examined. The tolerance limits ($\geq$90%) for both Pd(II) and Rh(III) ions were found to be 75,000 mg L^{-1} Na(I), 75,000 mg L^{-1} K(I), 50,000 mg L^{-1} Mg(II) and 50,000 mg L^{-1} Ca(II). A 30 s contact time was enough for both adsorption and elution. A preconcentration factor of 100 was obtained by using 100 mg of the nano sponge Mn_2O_3. The reusability of the adsorbent was 120 times. Adsorption capacities for Pd(II) and Rh(III) were found to be 42 and 6.2 mg g^{-1}, respectively. The detection limits were 1.0 μg L^{-1} for Pd(II) and 0.37 μg L^{-1} for Rh(III) and the relative standard deviations (RSD, %) were found to be $\leq$2.5%. The method was validated by analyzing the standard reference material, SRM 2556 (Used Auto Catalyst Pellets) and spiked real samples. The optimized method was applied for the preconcentration of Pd(II) and Rh(III) ions in water (sea water and wastewater), rock, street sediment and catalytic converter samples.

1. Introduction

Approximately 73% of the world production of rhodium is consumed in the production of autocatalysts [1]. Palladium is one of the noble metals and possesses attractive physical and chemical properties such as high melting point, corrosion resistance and extraordinary catalytic properties. It has found vital importance in many different, ordinary and advanced fields of industry, such as in jewellery and ornaments, electronics, telephone circuits, heat and corrosion resistance apparatus, catalysts and dental alloys [2,3].

Human exposure to particulates from traffic is of increasing importance. Converters contain platinum, palladium and rhodium in different combinations, which reduce the emission levels of toxic gas pollutants into the environment. Platinum metals are emitted from vehicle catalysts mostly (Pt > 95%, Pd > 85%, and Rh > 90%) as nanocrystalline particles attached to the Al_2O_3 support [4]. The platinum group elements(PGE) emissions are thought to occur mainly as a fine particulate material that originates from the abrasion and deterioration of the surface of the catalyst [4,5]. Once dispersed into the atmosphere they can be deposited on solid air suspended matter, transported for long distances, and gradually removed by wet and dry deposition as road dust, in aquatic environments, and on plants, soils, and sediments. The occurrence of fine dispersed particles, in particular easily bioavailable nanometer particles, generates problems with their inhalation and entering the respiratory tract (lungs, trachea) [6]. Many PGE compounds are known as potent respiratory allergens that can lead to rhinitis, conjunctivitis, asthma and urticaria [5]. Excessive exposure to palladium causes adverse health effects in humans such as primary skin problems, eye irritations, substantial degradation of DNA, and cell mitochondria, aggravation of hydroxyl radical damage and inhibition of enzyme activity [7]. For these reasons, there is a need to develop a method for the determination of precious metals at trace levels in more complicated geological and environmental matrices.

Solid phase extraction has become increasingly popular for the determination of trace levels of noble metals in various matrices. This method is simple, rapid and efficient with a high preconcentration factor compared to other separation techniques [8,9]. Nanomaterials as adsorbents, with physical features of less than 100 nm in one or more dimensions, have attracted considerable attention from scientists in recent years, mainly due to their unique, attractive, thermal, mechanical, electronic and biological properties. Nanosized structures may be in the form of particles, pores, wires or tubes [10]. One of the specific properties of nanomaterials is that a high percentage of the atoms of the nanoparticle are on the surface. The surface atoms are unsaturated and can therefore bind with other atoms, and they possess highly chemical activity [11–13]. Nanoparticles, due to their intrinsic surface

* Corresponding author. Tel.: +90 352 207 66 66; fax: +90 352 437 49 33.
E-mail address: serifet@erciyes.edu.tr (Ş. Tokalıoğlu).

http://dx.doi.org/10.1016/j.talanta.2014.04.027
0039-9140/

reactivity, high surface areas and high adsorption capacity, can adsorb many substances, such as metal ions and polar organic substances with a great adsorption speed [11,14–16]. Moreover the preparation of these adsorbents is very simple and inexpensive when compared with other commercially available solid-phase materials. In recent years, numerous nanometer-sized materials have been proposed and applied as solid phase extractants in the preconcentration of trace metals, such as TiO_2 [11,15,17,18], alumina [19,20], ZrO_2 [21], B_2O_3/TiO_2 composite [22], Schiff base-functionalized Fe_3O_4/SiO_2 [23], ultralayered Co_3O_4 [24], and graphene/Co_3O_4 composite [25]. Nanosize manganese oxides are of special interest because of their variable oxidation states and their wide applications in batteries, catalysis and chemical synthesis [26].

To our literature knowledge, no report has as yet been published about the use of nano sponge Mn_2O_3 as an adsorbent for the solid phase extraction of metal ions. In this work, nano sponge Mn_2O_3 was synthesized, characterized and used as a solid phase extractor for the separation and preconcentration of palladium and rhodium in various samples (sea water, wastewater, rock, catalytic converter and street sediment). Experimental parameters affecting the preconcentration of palladium and rhodium such as pH, adsorption and elution contact times, centrifuge rate and time, eluent type, concentration and volume, sample volume, adsorption capacity and matrix effects were studied and optimized.

2. Experimental

2.1. Instrumentation

Crystalline phase analysis of materials was made from the powder X-ray diffraction (XRD, BRUKER AXS D8 Advance) using Cu Kα radiation (λ=0.15406 nm) in the range of 2θ=10–90°. The morphology was measured by scanning electron microscopy (SEM, LEO 440 and Zeiss EVO LS 10 Lab6) with an accelerating voltage of 20 kV. The Brunauer–Emmet–Teller (BET) nitrogen adsorption–desorption analysis was conducted on a Micromeritics Gemini VII instrument.

A Perkin Elmer AAnalyst 800 model atomic absorption spectrometer (Waltham, MA, USA) equipped with palladium and rhodium hollow cathode lamps and a transversally heated graphite atomizer with an AS 800 autosampler was used for the determination of palladium and rhodium. Measurements (such as wavelength and spectral bandwidth) were carried out at 244.8 and 0.2 nm, 343.5 and 0.2 nm for Pd and Rh, respectively. The lamp currents were set at 30 mA for Pd and 20 mA for Rh. The acetylene/air flow rate was 2.0/17 L min^{-1}. A graphite furnace with an automatic sampler was used for the determination of Pd and Rh in street sediment samples. Aliquots of 10 μL of sample and calibration solutions were injected into pyrolytically coated graphite tubes. The signals were measured as peak area. The graphite furnace temperature program for Pd and Rh was operated according to the manufacturer's recommendations. The pH measurements were carried out on a Mettler Toledo 320 pH meter. A Wiggen Hauser vortex mixer for mixing samples and an Annita ALC PK120 model centrifuge for centrifuging of samples were used throughout all the experiments.

2.2. Reagents and solutions

All reagents were of analytical grade, unless otherwise stated. All solutions were prepared by using ultra-high purity water from a Milli-Q system (18.2 MΩ cm). Working standard solutions of Pd(II) and Rh(III) were prepared by dilution of their 1000 mg L^{-1} single element stock solutions (Sigma-Aldrich). Different buffer solutions, H_3PO_4/NaH_2PO_4 for pH 2 and 3, CH_3COOH/CH_3COONa for pH 4–6.5, CH_3COONH_4 for pH 7 and 7.5 and NH_3/NH_4Cl for pH 8 and 9 were used in the experiments. The salts of interfering ions used for matrix effect studies were obtained from Merck. Diluted HNO_3 (Merck, 65%) and HCl (Merck, 37%) were tested as eluent.

2.3. Synthesis of nano sponge Mn_2O_3

The nano sponge Mn_2O_3 was firstly prepared by a glycine-nitrate combustion process in our research laboratory. Stoichometric amounts of $Mn(CH_3COO)_2 \cdot 4H_2O$(Sigma) were dissolved in distilled water under stirring. After a transparent solution was formed, glycine (Merck) was added to the mixture either as a solid or as a water solution. Its role was to serve both as a fuel for combustion and as a complexant to prevent inhomogeneous precipitation of individual components prior to combustion. Finally, nitric acid with a 1:1 mol ratio of nitrate to acetate anions was added to the solution. The molar ratio of glycine to nitrate was 1:4. The solution was heated continuously without any previous thermal dehydration. Afterwards the solution became a transparent viscous gel which auto-ignited automatically, giving a voluminous, black, sponge-like ash combustion product. The resulting ash was heated at 300 °C for 1 h.

2.4. General procedure

The pH of the model solution of 20 mL containing 100 mg nano sponge Mn_2O_3, 8 μg Pd(II) and 4 μg Rh(III) in a 50 mL centrifuge tube was adjusted to 6 by aid of the relevant buffer solution. After 30 s vortexing, the mixture was centrifuged at 3500 rpm for 3 min. The supernatant liquid was discarded. For the elution of retained Pd(II) and Rh(III) ions, 2 mL of 2 mol L^{-1} HCl was added to the centrifuge tube. After 30 s vortexing and then centrifuging at 3500 rpm for 3 min, the analytes in the eluate were determined by flame atomic absorption spectrometry (FAAS).

2.5. Sample preparation

Wastewater and street sediment samples were collected from the Kayseri City Organized Industrial Region (Turkey). Sea water samples were collected from the Aegean Sea (Izmir, Turkey). The water samples were filtered through a 0.45 μm membrane filter and acidified with concentrated HNO_3. One hundred fifty milliliter water samples were used for the analysis of Pd and Rh. The rock, converter and street sediment samples were dried at 100 °C for 2 h and then ground.

Portions of 0.10 g of street sediment and of 0.10 g of rock sample were transferred into 100 mL beakers and two portions of 10 mL aqua regia were added. The mixture was evaporated almost to dryness. The insoluble part was filtered through a blue band filter paper using ultra-high purity water [24]. The filtrate was diluted to a volume of 20 mL with ultra-high purity water and submitted to the preconcentration procedure for the determination of Pd and Rh. The determination of analytes in the street sediment samples was performed by using GFAAS.

For the analysis, 0.010 g of catalytic converter sample, and 0.025 g of standard reference material 2556 (Used Auto Catalyst Pellets) were used. The SRM 2556 and converter sample were calcined in an oven for 2 h at 500 °C prior to analysis to assure a stable weighing form. The catalytic converter sample and SRM 2556 were put into 100 mL teflon beakers. Then 10 mL of aqua regia was added to the beaker. The mixture was evaporated near to dryness. Ten milliliters of aqua regia was again added to the beaker and it was again evaporated near to dryness. Then 3 mL concentrated hydrofluoric acid was added to the residue [27]. After evaporation, the residue was filtered through a blue band filter paper by washing with ultra-high purity water and the volume of the filtrate was made up to 20 mL. The pH of the filtrate was adjusted to 6 and the preconcentration procedure described above was applied.

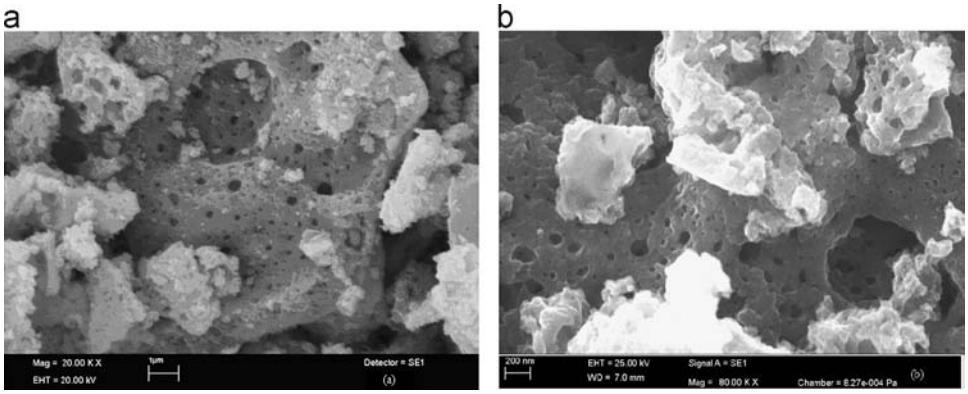

Fig. 1. Electron micrographs of nano sponge Mn_2O_3 synthesized by combustion process (a) low and (b) high magnification.

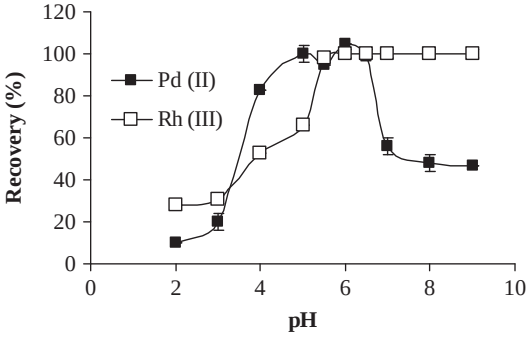

Fig. 2. Effect of pH on the Pd(II) and Rh(III) recovery.

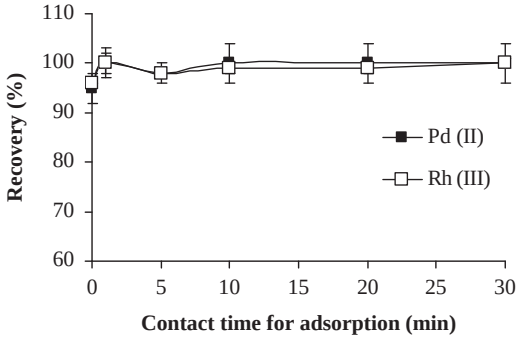

Fig. 3. Effect of contact time on recovery of Pd(II) and Rh(III).

3. Results and discussion

3.1. Characterization of nano sponge Mn_2O_3

The XRD pattern of the final product is shown in Fig. S1. All of the diffraction peaks in this pattern could be assigned to a pure cubic phase of Mn_2O_3, which is in a good agreement with the standard values (JCPDS: 41-1442). No peaks of impurities can be detected from this pattern. The average size of the nanocrystallites was also estimated by using the Debye–Scherrer formula [28]; $D=0.9\lambda/(\beta\cos\theta)$, where λ, β and θ are the X-ray wavelength, the full width at half maximum (FWHM) of the diffraction peak and the Bragg diffraction angle respectively. The estimated crystallite size was found to be 31 nm from XRD data.

Scanning electron micrographs of the Mn_2O_3 powders are shown in Fig. 1. It is obvious that the Mn_2O_3 powders have a spherical morphology in the primary particles and the estimated particle size is about 50–100 nm in diameter, while the primary particles are densely agglomerated in secondary forms. Fig. 1 depicts the typical morphologies of the combusted powders which are characteristic of a mesoporous structure with uniformly distributed inter connected pores.

N_2 adsorption/desorption isotherms were employed to investigate the specific surface area of the Mn_2O_3 nanoparticles, as shown in Fig. S2. The BET surface area and pore size for Mn_2O_3 were determined to be 6.6 m^2/g and 55.1 nm, respectively.

3.2. Effect of pH

The solution pH is one of the main parameters because it influences the distribution of active sites on the surface of the nano sponge Mn_2O_3. Therefore, the effect of the initial solution pH on the adsorption of Pd(II) and Rh(III) was investigated in the pH range of 2–9 by using model solutions of 20 mL containing 100 mg nano sponge Mn_2O_3, 8 μg Pd(II) and 4 μg Rh(III). Two milliliters of 2 mol L^{-1} HCl was used for the elution of retained Pd(II) and Rh (III) ions. The changes in recovery values for Pd(II) and Rh(III) with the pH of the solution are shown in Fig. 2. The results show that the quantitative recovery pH ranges were 5–6.5 for Pd(II) and 5.5–9 for Rh(III). The adsorption of metal ions at low pH values ($pH \leq 5.5$) was low because of the protonation of oxygen atoms bound to the manganese. The recovery value of Pd(II) decreased rapidly when the pH was ≥ 7. Because $Pd(OH)_2$ precipitation occurs in high pH values, which reduces the amount of Pd(II) ions to be able to interact with the sorbent [29]. Therefore pH 6 was selected for subsequent experiments.

3.3. Effect of contact times on adsorption and elution

In order to determine the adsorption and elution equilibrium time, the effect of contact time between Mn_2O_3 nano sponge and model solutions containing 8 μg Pd(II) and 4 μg Rh(III) adjusted to pH 6 was examined. The adsorption and elution contact times of 10 s, 0 (30 s), 1, 5, 10, 20 and 30 min were studied. The experimental results for adsorption contact time are given in Fig. 3. The recovery values of Pd(II) and Rh(III) for both adsorption and elution were quantitative for all the contact times, except for 10 s. The contact time of only 30 s was found to be sufficient to reach equilibrium ($R\%=95$–97). This means that the adsorption and elution kinetic for Pd(II) and Rh(III) are very rapid. This can be attributed to the high surface reactivity of the adsorbent. Therefore, the contact time of 30 s for both adsorption and elution was used in further experiments.

3.4. Effect of centrifugation rate and time

Centrifugation rate and time are important parameters in view of the rapidity of the method and phase separation. Therefore, the centrifuge speed was investigated at between 2000 and 4000 rpm for 5 min. Because the phase separation was not sufficient at 2000 and 2500 rpm, 3500 rpm was used in subsequent experiments. The centrifugation time in the range of 1–5 min at 3500 rpm was investigated. The obtained results were found to be quantitative for 2–5 min ($R\%$=96–100). The phase separation was not sufficient at the centrifuge time of 1 min. Therefore, 3 min was chosen as optimal time.

3.5. Effect of eluent type, concentration and volume

In order to elute the Pd(II) and Rh(III) adsorbed on the nano sponge Mn_2O_3, diluted HNO_3 and diluted HCl were used in different concentrations (0.5, 1, 1.5, 2, 2.5 mol L^{-1}). The results are given in Table 1. As can be seen, the recoveries of Pd(II) and Rh (III) were quantitative when 2 mL of 2 mol L^{-1} HNO_3, 2.5 mol L^{-1} HNO_3, 2 mol L^{-1} HCl, and 2.5 mol L^{-1} HCl solutions were used. Due to the formation of anionic chloro complexes of Pd(II) and Rh(III), 2 mol L^{-1} HCl was selected for the experiments. The effect of the volume of HCl on the recoveries of Pd(II) and Rh(III) was investigated for 2, 4, 6, 8, and 10 mL eluent volumes. For all the volumes of 2 mol L^{-1} HCl, the recovery values of Pd(II) and Rh(III) changed in the range of 97–103%. To obtain a high preconcentration factor, 2 mL eluent volume was used in all the experiments.

Table 1
Effect of concentration of HNO_3 and HCl on the recovery of Pd(II) and Rh(III), eluent volume: 2 mL, n=3.

Conc. of HNO_3 (mol L^{-1})	R (%) ± SD		Conc. of HCl (mol L^{-1})	R (%) ± SD	
	Pd(II)	Rh(III)		Pd(II)	Rh(III)
0.5	55 ± 3	48 ± 1	0.5	77 ± 3	60 ± 0
1.0	80 ± 3	58 ± 0	1.0	75 ± 3	66 ± 1
1.5	86 ± 3	64 ± 1	1.5	94 ± 3	86 ± 1
2.0	98 ± 0	98 ± 1	2.0	96 ± 0	100 ± 2
2.5	100 ± 0	99 ± 1	2.5	98 ± 0	98 ± 1

3.6. Effect of sample volume

The effect of sample volume on the recovery of Pd(II) and Rh (III) was investigated by using the model solutions of 20, 100, 150, 200, 250 and 300 mL containing 8 μg Pd(II) and 4 μg Rh(III) and the above mentioned preconcentration method was applied. The Pd(II) and Rh(III) concentrations in these solutions were 0.4 and 0.2, 0.08 and 0.04, 0.05 and 0.03, 0.04 and 0.02, 0.03 and 0.016, 0.027 and 0.013 mg L^{-1}, respectively. The recovery values for Pd(II) and Rh(III) were found to be in the range 90–100% up to 200 mL of sample volume. The preconcentration factor was obtained as 100 for Pd(II) and Rh(III) due to the elution volume of 2 mL.

3.7. Reusability of the adsorbent

The stability and regeneration of the nano sponge Mn_2O_3 were investigated by using the described preconcentration method. A series of adsorption/desorption experiments were performed to understand the reusability of the Mn_2O_3. The adsorbent was reused after being regenerated with 2 mL of 2 mol L^{-1} HCl and then 5 mL of ultra-high purity water, respectively. It was stored in ultra-high purity water when it was not in use. The stability of sorbent was excellent. The recovery results show that the adsorbent could be reused up to 120 times without a decrease in the recoveries.

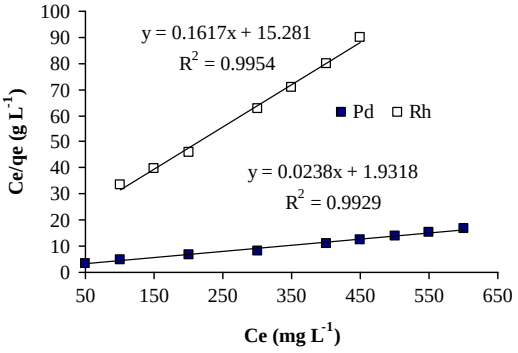

Fig. 4. Linearized Langmuir adsorption of Pd(II) and Rh(III) on nano sponge Mn_2O_3.

Table 2
Effect of some matrix ions on the recoveries of Pd(II) and Rh(III) (n=3).

Ion	Salt	Tolerable concentration, (mg L^{-1}) for Pd(II)	Pd(II) R ± SD (%)	Tolerable concentration, (mg L^{-1}) for Rh(III)	Rh(III) R ± SD (%)
Na(I)	NaCl	75,000	91 ± 2	75,000	90 ± 2
K(I)	KNO_3	75,000	89 ± 2	100,000	92 ± 2
Mg(II)	$Mg(NO_3)_2 \cdot 6H_2O$	50,000	102 ± 2	75,000	93 ± 0
Ca(II)	$Ca(NO_3)_2 \cdot 6H_2O$	50,000	97 ± 0	50,000	97 ± 0
Cu(II)	$Cu(NO_3)_2 \cdot 5H_2O$	50	95 ± 3	100	98 ± 2
Al(III)	$Al(NO_3)_3 \cdot 9H_2O$	100	90 ± 2	100	100 ± 0
Ni(II)	$NiCl_2 \cdot 6H_2O$	25	97 ± 3	50	93 ± 0
Cd(II)	$Cd(NO_3)_2 \cdot 4H_2O$	50	94 ± 0	100	100 ± 2
Co(II)	$Co(NO_3)_2 \cdot 6H_2O$	25	97 ± 3	50	92 ± 3
Fe(III)	$Fe(NO_3)_3 \cdot 9H_2O$	25	97 ± 3	50	92 ± 3
Pb(II)	$Pb(NO_3)_2$	25	97 ± 3	100	98 ± 2
Cr(III)	$Cr(NO_3)_3 \cdot 9H_2O$	25	97 ± 3	10	100 ± 2
Zn(II)	$Zn(NO_3)_2 \cdot 6H_2O$	50	92 ± 3	50	91 ± 2
F^-	NaF	2500	100 ± 2	500	90 ± 2
SO_4^{2-}	Na_2SO_4	500	90 ± 4	1000	98 ± 2
PO_4^{2-}	Na_3PO_4	250	94 ± 0	250	92 ± 2
CO_3^{2-}	Na_2CO_3	2500	95 ± 2	10	94 ± 2

3.8. Effect of interferences

In order to investigate the effect of various cations and anions found in natural samples, alkaline, alkaline earth and transition metal ions at increasing concentrations were added to 20 mL of model solution containing 8 μg Pd(II) and 4 μg Rh(III). After the preconcentration method was applied, the recovery values for Pd (II) and Rh(III) were calculated. The results are presented in Table 2. The tolerance limit (TL), which is the matrix ion concentration making ≥90% recovery values of Pd(II) and Rh(III), was found to be rather high. TLs for both metal ions are 75,000 mg L^{-1} for Na(I) and K(I), 50,000 mg L^{-1} for Mg(II) and Ca(II), 100 mg L^{-1} for Al(III), 50 mg L^{-1} for Cu(II), Cd(II) and Zn(II), 25 mg L^{-1} for Ni(II), Co(II), Fe(III), and Pb(II), 10 mg L^{-1} for Cr(III), 500 mg L^{-1} for F^- and SO_4^{2-}, 250 mg L^{-1} for PO_4^{3-} and 10 mg L^{-1} for CO_3^{2-}. As can be seen from Table 2, the tolerance limits for Rh(III) are generally higher than those of Pd(II). These results show that Pd(II) and Rh(III) can be successfully determined in complex matrices.

Table 3
The analysis results of standard reference material.

Element	SRM 2556 (used auto catalyst pellets)[a]		
	Certified[b] (μg g^{-1})	Found[c] (μg g^{-1})	R (%)
Pd	326.0 ± 1.6	335.2 ± 8.8	103
Rh	51.2 ± 3.8	53.5 ± 3.9	104

[a] The main component of the matrix is Al (40%). Ca (0.1%), Ce (1%), Fe (0.8%), La (0.7%) and Si (0.2%) are present at a relatively high concentration, as well as Ba (100 mg g^{-1}), Zn (600 mg g^{-1}), Zr (300 mg g^{-1}), Pb (6228 mg g^{-1}), Pt (697.4 mg g^{-1}).
[b] At 99% confidence level.
[c] $\bar{x} \pm SD$, $n=3$.

Table 4
Determination of Pd(II) and Rh(III) in sea water and wastewater samples (sample volume: 150 mL, final volume: 2 mL).

Element	Sea water			Wastewater		
	Added (μg L^{-1})	Found[a] (μg L^{-1})	R (%)	Added (μg L^{-1})	Found[a] (μg L^{-1})	R (%)
Pd(II)	–	nd[b]		–	nd	
	6.7	6.8 ± 0	102	6.7	6.2 ± 0	93
	13.3	13.8 ± 0.2	104	13.3	13.4 ± 1.2	101
Rh(III)	–	nd		–	nd	
	6.7	6.6 ± 0.9	98	6.7	6.5 ± 0.9	98
	13.3	13.6 ± 0.9	102	13.3	14.5 ± 0.9	109

[a] $\bar{x} \pm SD$, $n=3$.
[b] nd: not detected.

3.9. Adsorption capacity of the nano sponge Mn_2O_3

The capacity of nano sponge Mn_2O_3 for adsorption of Pd(II) and Rh(III) was studied by using 20 mL of model solutions containing 100 mg adsorbent, 50–600 mg L^{-1} of Pd(II) and 100–450 mg L^{-1} of Rh(III) at pH 6. The eluent was diluted 50 or 250 fold. As shown in Fig. 4, the experimental adsorption data were applied to the Langmuir equation to evaluate the maximum adsorption capacity of the adsorbent [24,30].

$$\frac{C_e}{q_e} = \left(\frac{1}{K_L q_m}\right) + \left(\frac{C_e}{q_m}\right)$$

where q_e and C_e are the amount adsorbed (mg g^{-1}) and the Pd(II) and Rh(III) concentration in solution (mg L^{-1}), respectively, at equilibrium. K_L is the Langmuir constant (L mg^{-1}) and q_m is the maximum adsorption capacity of the adsorbent (mg g^{-1}). The Langmuir isotherm was used to determine the q_m and K_L values from the linear coefficients obtained by plotting C_e/q_e as a function of C_e. The adsorption capacities of Pd(II) and Rh(III) were found to be 42 and 6.2 mg g^{-1}, respectively. The Langmuir constant was 0.0123 L mg^{-1} for Pd(II) and 0.0106 L mg^{-1} for Rh(III).

3.10. Analytical figures of merits

The calibration curves of Pd(II) and Rh(III) were linear in the concentration ranges of 1–10 mg L^{-1} by using FAAS without the preconcentration method with regression coefficients (r^2) of 0.9997 and 0.9998, respectively. The linear ranges obtained by using GFAAS without the preconcentration method were 1–10 μg L^{-1} for Pd(II) ($r^2=0.9991$) and 2.5–20 μg L^{-1} for Rh(III) ($r^2=0.9987$). The detection limits (DLs) of Pd(II) and Rh(III) without the preconcentration procedure for 2 mol L^{-1} HCl were found to be 0.25 and 0.12 mg L^{-1} for FAAS and 0.34 and 0.19 μg L^{-1} for GFAAS, respectively. These results were obtained according to the equation $3s/b$, where s is the standard deviation of the blank signals ($n=8$) and b is the slope of the linear calibration graph.

The calibration curves obtained using FAAS for the standard solutions preconcentrated by the proposed solid phase extraction method were linear in the concentration ranges of 12.5–500 μg L^{-1} in the initial solutions of Pd(II) and Rh(III) with $A=0.0052[Pd]+0.0003$ ($r^2=0.9994$) and $A=0.008[Rh]-0.0004$ ($r^2=0.9996$). The equations were given for Pd(II) and Rh(III) concentrations in the final solutions after the preconcentration. The calibration data obtained using GFAAS with the preconcentration method were linear in the ranges of 0.05–0.5 μg L^{-1} for Pd(II) and 0.025–0.75 μg L^{-1} for Rh(III) in the initial solutions. The equations of calibration graphs for Pd(II) and Rh(III) concentration in the final solutions were found to be $A=0.0083[Pd]+0.0022$ ($r^2=0.9973$) and $A=0.0049[Rh]+0.0011$ ($r^2=0.9992$), respectively. For the determination of DLs of the described method, the method was applied to the blank solutions

Table 5
Determination of Pd(II) and Rh(III) in rock, converter and street sediment samples (final volume: 2 mL).

Element	Rock			Converter			Street sediment[a]		
	Added (μg g^{-1})	Found[b] (μg g^{-1})	R (%)	Added (μg g^{-1})	Found[b] (μg g^{-1})	R (%)	Added (ng g^{-1})	Found[b] (ng g^{-1})	R (%)
Pd(II)	–	37.4 ± 2.3		–	671 ± 12		–	46.7 ± 1.9	–
	20	56.3 ± 2.3	95	300	969 ± 0	99	20	66.3 ± 1.7	95
	40	76.0 ± 2.3	97	600	1245 ± 12	96	40	84.9 ± 1.6	95
Rh(III)	–	21.6 ± 1.5		–	48.3 ± 0		–	50.3 ± 0.9	
	20	41.4 ± 2.0	99	50	95.7 ± 8.2	95	50	98.4 ± 4.1	96
	40	59.4 ± 0.8	95	100	143 ± 8	95	100	147 ± 1	97

[a] The analysis was made by GFAAS after applying the described method.
[b] $\bar{x} \pm SD$, $n=3$.

Table 6
Comparison of the present method with some solid phase extraction methods reported in literature for Pd(II) and Rh(III) preconcentration.

Adsorbent/technique	Element	pH	AC[a] (mg g^{-1})	PF[b]	DL[c] (μg L^{-1})	RSD (%)	Contact time (min)	Reusability	Sample	Refs
Ion imprinted polymers/FAAS	Pd	6	9.25–13.3	33	5	3		100	Spiked tap water	[3]
Fe_3O_4 nanoparticles/ICP-AES	Pd, Rh	2.5	11.0, 15.3				30			[11]
Modifed multiwalled carbon nanotubes/FAAS	Rh	3.7	6.6	120	0.01	0.97		50	Tap, well, river, sea and waste water, platinum–iridium alloy	[31]
Microcrystalline naphthalene/ spectrophotometry	Rh	3.3–5.8			20	1.2			Various synthetic samples	[32]
Ion imprinted polymer/ resonance light-scattering	Rh	6	14.5	10	0.024	< 3.0		20	Water, alloy, catalyst	[33]
Functionalized Amberlite XAD-4/ICP-AES	Rh	6.5	26.3	10	50	4.1	7 h	10	Tap water	[34]
Magnetic Fe_3O_4 nano particles/FAAS	Pd, Rh	10.5	27.2, 31.8	150	2.9, 1.4	1.9, 1.7	2		Platinum–iridium alloy, road dust	[35]
Nanometer sized alumina modified by QAHBA/ FI-ICP-OES[d]	Pd	4.5–6.5	7.6	10	0.44	2.3	4	30	Natural water samples	[36]
Nano sponge Mn_2O_3/FAAS	Pd, Rh	6	42, 6.2	100	1.0, 0.37	2.5, 1.0	30 s	120	Sea water, wastewater, rock, converter, street sediment	This work

[a] AC: adsorption capacity.
[b] PF: preconcentration factor.
[c] DL: detection limit.
[d] QAHBA: 3-(8-quinolinylazo)-4-hydroxybenzoic acid.

($n=10$) at the optimal experimental conditions before the measurement by FAAS and GFAAS. The DLs of the method based on $3s/b$ definition using FAAS (with a preconcentration factor of 100-fold) and GFAAS were found to be 1.0 and 0.011 μg L^{-1} for Pd(II) and 0.37 and 0.013 μg L^{-1} for Rh(III), respectively.

The precision (as RSD, %) of the described method under the optimal conditions using FAAS was determined by 9 replicates of model solutions containing 0.4 and 0.05 mg L^{-1} for Pd(II) and 0.2 and 0.05 mg L^{-1} for Rh(III). It was calculated to be 2.5 and 5.8% for Pd(II) and 1.0 and 4.8% for Rh(III). The precision experiment of the described method for GFAAS was also performed by using model solutions ($n=9$) containing 0.05 μg L^{-1} Pd(II) and 0.05 μg L^{-1} Rh. The RSD(%) values were found to be 5.6% for Pd(II) and 5.1% for Rh(III).

3.11. Accuracy of the method and analysis of real samples

The described method was validated by analysis of a standard reference material, SRM 2556 (Used Auto Catalyst Pellets) and also by recovery studies in real samples. The obtained results are in good agreement with the certified values (see Table 3). The method was applied for the preconcentration of Pd(II) and Rh(III) in sea water, wastewater, rock, street sediment, and catalytic converter samples with recovery experiments. For this purpose, known amounts of the metal ions were added to 150 mL of the water samples, 0.10 g of street sediment, 0.10 g of rock sample and 0.010 g of catalytic converter sample. The results obtained after applying the described method are given in Tables 4 and 5. The recovery values of Pd(II) and Rh(III) in the samples were found to be in the range of 93–109%. This means that the method can be successfully applied to a wide variety of samples with complex matrices.

3.12. Comparison with other methods

A comparison of the described solid phase extraction method with other methods for the separation and determination of Pd(II) and Rh(III) is given in Table 6. In comparison with the other reported methods, the present method generally shows a high preconcentration factor (100), short equilibrium time (30 s) and high reusability of the adsorbent (120 times). The adsorption capacity for Pd(II) (42 mg g^{-1}) is higher than those of the other methods. The detection limit of the method and precision are comparable and/or better than those of the other methods. The applicability of the method for the various sample matrices is excellent due to its very high tolerance limits.

4. Conclusions

In this work, a new adsorbent (Mn_2O_3) was successfully synthesized and characterized by XRD, SEM and BET analyses. The adsorbent was used for the first time for the solid phase extraction of Pd(III) and Rh(III) in various samples. The developed method is simple, rapid, precise, accurate, reliable and environmentally friendly. The cost of the adsorbent is low and it has a rather rapid adsorption and elution kinetic. The adsorption and elution time of Pd(II) and Rh(III) ions are only 30 s. The acidic working pH (6), good precision ($\leq 2.5\%$) and low detection limits (1.0 and 0.37 μg L^{-1}) are the other important properties of the method. The method can be used easily for Pd(II) and Rh(III) preconcentration from sea water, wastewater, rock, street sediment and catalytic converter samples in routine analysis laboratories.

Appendix A. Supplementary material

Supplementary data associated with this article can be found in the online version at http://dx.doi.org/10.1016/j.talanta.2014.04.027.

References

[1] F.S. Rojas, C.B. Ojeda, J.M.C. Pavón, Talanta 64 (2004) 230–236.
[2] R. Li, Q. He, Z. Hu, S. Zhang, L. Zhang, X. Chang, Anal. Chim. Acta 713 (2012) 136–144.
[3] B.G. Zyłkiewicz, B. Lesniewska, I. Wawreniuk, Talanta 83 (2010) 596–604.
[4] C. Colombo, A.J. Monhemius, J.A. Plant, Ecotox. Environ. Safe. 71 (2008) 722–730.
[5] W.H. Hsua, S.J. Jianga, A.C. Sahayam, Anal. Chim. Acta 794 (2013) 15–19.
[6] M. Balcerzak, Crit. Rev. Anal. Chem. 41 (2011) 214–235.
[7] R.K. Sharma, A. Pandey, S. Gulati, A. Adholeya, J. Hazard. Mater. 209–210 (2012) 285–292.
[8] Y. Li, Y.F. Huang, Y. Jiang, B.L. Tian, F. Han, X.P. Yan, Anal. Chim. Acta 692 (2011) 42–49.

[9] H. Ebrahimzadeh, N. Tavassoli, M.M. Amini, Y. Fazaeli, H. Abedi, Talanta 81 (2010) 1183–1188.
[10] K. Pyrzynska, Trends Anal. Chem. 43 (2013) 100–108.
[11] A. Uheida, M. Iglesias, C. Fontás, M. Hidalgo, V. Salvadó, Y. Zhang, M. Muhammed, J. Colloid Interface Sci. 301 (2006) 402–408.
[12] R. Liu, P. Liang, J. Hazard. Mater. 152 (2008) 166–171.
[13] A.R. Türker, Sep. Purif. Technol. 41 (2012) 169–206.
[14] A.E. Karatapanis, D.E. Petrakis, C.D. Stalikas, Anal. Chim. Acta 726 (2012) 22–27.
[15] L. Zhang, Y. Wang, X. Guo, Z. Yuan, Z. Zhao, Hydrometallurgy 95 (2009) 92–95.
[16] V.A. Lemos, L.S.G. Teixeira, M. de A. Bezerra, A.C.S. Costa, J.T. Castro, L.A.M. Cardoso, D.S. de Jesus, E.S. Santos, P.X. Baliza, L.N. Santos, Appl. Spectrosc. Rev. 43 (2008) 303–334.
[17] S. Chen, S. Zhu, D. Lu, Microchem. J. 110 (2013) 89–93.
[18] M. Amjadi, A. Samadi, Colloid Surf. A 434 (2013) 171–177.
[19] J.L. Manzoori, M. Amjadi, M. Darvishnejad, Microchim. Acta 176 (2012) 437–443.
[20] M. Ezoddin, F. Shemirani, K.h. Abdi, M.K. Saghezchi, M.R. Jamali, J. Hazard. Mater. 178 (2010) 900–905.
[21] J.S. Suleiman, B. Hu, X. Pu, C. Huang, Z. Jiang, Microchim. Acta 159 (2007) 379–385.
[22] O.M. Kalfa, Ö. Yalçınkaya, A.R. Türker, J. Hazard. Mater. 166 (2009) 455–461.
[23] H. Bagheri, A. Afkhami, M.S. S-Tehrani, H. Khoshsafar, Talanta 97 (2012) 87–95.
[24] E. Yavuz, Ş. Tokalıoğlu, H. Şahan, Ş. Patat, Talanta 115 (2013) 724–729.
[25] E. Yavuz, Ş. Tokalıoğlu, H. Şahan, Ş. Patat, RSC Adv. 3 (2013) 24650–24657.
[26] N. Chandra, S. Bhasin, M. Sharma, D. Pal, Mater. Lett. 61 (2007) 3728–3732.
[27] J. Fang, L.W. Liu, X.P. Yan, Spectrochim. Acta B 61 (2006) 864–869.
[28] L.V. Azarof., M.J. Buerger, The Powder Method in X-ray Crystallography, first ed., McGraw-Hill, New York, 1958.
[29] T. Çetin, Ş. Tokalıoğlu, A. Ülgen, S. Şahan, İ. Özentürk, C. Soykan, Talanta 105 (2013) 340–346.
[30] M.M. Bekheit, N. Nawar, A.W. Addison, D.A. A.-Latif, M. Monier, Int. J. Biol. Macromol. 48 (2011) 558–565.
[31] S. Ghaseminezhad, D. Afzali, M.A. Taher, Talanta 80 (2009) 168–172.
[32] M.A. Taher, Anal. Chim. Acta 382 (1999) 339–344.
[33] B. Yang, T. Zhang, W. Tan, P. Liu, Z. Ding, Q. Cao, Talanta 105 (2013) 124–130.
[34] H.A. Panahi, H.S. Kalal, E. Moniri, M.N. Nezhati, M.T. Menderjani, S.R. Kelahrodi, Microchem. J. 93 (2009) 49–54.
[35] S.Z. Mohammadia, M.A. Karimia, H. Hamidiana, Y.M. Baghelani, L. Karimzadeha, Sci. Iran 18 (2011) 1636–1642.
[36] C.Z. Hang, B. Hu, Z.C. Jiang, N. Zhang, Talanta 71 (2007) 1239–1245.